

Density profiles of small Dirac operator eigenvalues for two color QCD at nonzero chemical potential compared to matrix models

Gernot Akemann^{ab}, Elmar Bittner^c, Maria-Paola Lombardo^d, Harald Markum^e, Rainer Pullirsch^e

^aService de Physique Théorique, CEA/DSM/SPhT Saclay, Unité associée CNRS/SPM/URA 2306, F-91191 Gif-sur-Yvette Cedex, France

^bDepartment of Mathematical Sciences, Brunel University West London, Uxbridge, UB8 3PH, UK

^cInstitut für Theoretische Physik, Universität Leipzig, Augustusplatz 10/11, D-04109 Leipzig, Germany

^dINFN-Laboratori Nazionali di Frascati, I-00044 Frascati, Italy

^eAtominstytut, Technische Universität Wien, A-1040 Wien, Austria

We investigate the eigenvalue spectrum of the staggered Dirac matrix in two color QCD at finite chemical potential. The profiles of complex eigenvalues close to the origin are compared to a complex generalization of the chiral Gaussian Symplectic Ensemble, confirming its predictions for weak and strong non-Hermiticity. They differ from the QCD symmetry class with three colors by a level repulsion from both the real and imaginary axis.

1. Introduction

The comparison of small Dirac operator eigenvalues from lattice QCD to matrix models has been very successful at zero chemical potential [1]. At $\mu \neq 0$ detailed comparisons to the microscopic Dirac operator origin spectrum have been few for two reasons. First, unquenched QCD suffers from a complex action problem and second, matrix model predictions were not available. Very recently substantial progress has been made for complex chiral matrix models. Quenched [2,3] and unquenched [4] predictions for QCD have been achieved, as well as results for adjoint gauge theories and staggered two color QCD [5]. They have been successfully tested for quenched QCD [6], and our aim is to extend these results to other symmetry classes. The advantage of SU(2) is to avoid the complex determinant of the action matrix [7]. Already a few years ago, we computed the lowest eigenvalues of the unquenched SU(2) Dirac operator at $\mu \neq 0$ [8], with low statistics though [9]. We redo the analysis as we can now compare to [5]. For simplicity we only present quenched results here.

2. Matrix model predictions

In Ref. [10] a complex chiral matrix model with the same global symmetries as QCD at $\mu \neq 0$ was introduced. Its microscopic Dirac spectrum was obtained only very recently [3,4], after previous asymptotic results in [2] for a related model. Although the presence of μ alters the chiral symmetry breaking patterns for SU(2) and the adjoint representation, the symmetry analysis of Dirac matrix elements being real, complex or quaternion remains valid [11]. Following the two-matrix model approach [4] new results for quaternionic matrices are now available [5]. We only reproduce the quenched microscopic density here and refer to Ref. [5] for more details.

In QCD at $\mu = 0$, the lowest Dirac eigenvalues scale with the volume $1/V$ to build up a finite condensate Σ according to the Banks-Casher relation. At weak non-Hermiticity, a concept first introduced in [12], this scaling remains unchanged [2]. The support of the density remains quasi one-dimensional as we send $\mu \rightarrow 0$, keeping $\lim_{N \rightarrow \infty} 2N\mu^2 \equiv \alpha^2$ fixed. Here $N \sim 2V$ is the size of the random matrix. In contrast to that, at strong non-Hermiticity the eigenvalues fill a two-

dimensional surface, and thus the scaling is modified to $\sim 1/\sqrt{V}$ [2]. The quenched microscopic density at weak non-Hermiticity in the sector of topological charge ν is reading [5]

$$\begin{aligned} \rho_w(\xi) &= \frac{|\xi|^2(\xi^{*2} - \xi^2)}{2^4(\pi\alpha^2)^2} K_{2\nu} \left(\frac{|\xi|^2}{\alpha^2} \right) e^{\frac{\xi^2 + \xi^{*2}}{2\alpha^2}} \quad (1) \\ &\times \int_0^1 ds \int_0^1 dt t^{-\frac{1}{2}} e^{-s(1+t)\alpha^2} \\ &\times (J_{2\nu}(2\sqrt{st}\xi)J_{2\nu}(2\sqrt{s}\xi^*) - (\xi \leftrightarrow \xi^*)). \end{aligned}$$

Here, we have rescaled the complex eigenvalues according to $\xi \sim Vz$.

The limit of strong non-Hermiticity can be obtained by taking the limit $\alpha \rightarrow \infty$ in Eq. (1). The resulting microscopic density is symmetric with respect to the axes $\Re(\xi)$ and $\Im(\xi)$.

The zero momentum sector of chiral perturbation theory with $\mu \neq 0$ contains two parameters [13], Σ and the decay constant f_π , with the relative rescaling between mass and μ term depending on the ratio only. In the weak limit Eq. (1) becomes a function of ξ/α only, by substituting $s\alpha^2 = r$. Note that the first integral then runs to α^2 . However, at small $\alpha \gtrsim 0$ this change of variables breaks down. The integral becomes approximately α -independent while the prefactor strongly varies with α . Thus in this regime eigenvalues z (or masses) and μ can be rescaled independently with *two* parameters.

3. Lattice data at $\mu \neq 0$

Our computations with gauge group $SU(2)$ on a 6^4 lattice at $\beta = 4/g^2 = 1.3$ have $N_f = 2$ flavors of staggered fermions. For this system the fermion determinant is real and lattice simulations of the full theory with chemical potential are feasible. To compare with the quenched predictions from above we have chosen a large value for the quark mass $ma = 20$ (a being the lattice spacing in physical units) that effectively quenches the theory. We have checked this by comparing to simulations with $ma = 2$, following exactly the same analytical curve as in Fig. 1 below. A phase transition occurs at $\mu_c \approx m_\pi/2 \approx 0.3$ where the chiral condensate goes to zero and a diquark condensate develops [7].

At strong gauge coupling and thus away from the continuum limit, staggered fermions have the disadvantage of shifting the (topological) Dirac zero modes and mixing them with the nonzero modes. We have accounted for this by setting $\nu = 0$ in Eq. (1) above. Only more sophisticated methods as improved actions [14] can recover topology in the staggered approach. We produced around 10000 configurations for two values of $\mu = 0.001$ and $\mu = 0.2$, corresponding to weakly and strongly non-Hermitian lattice Dirac operators, respectively.

Fig. 1 shows that the data agree very well to the functional form of Eq. (1) at weak non-Hermiticity. After normalizing histograms and formula to unity we rescale the lattice eigenvalues z by $\xi = \pi z/d$, with the spacing $d \propto 1/V$. The weak non-Hermiticity parameter α^2 has been rescaled with a second parameter $\sim f_\pi^2/d$ to match the data. In contrast to QCD with three colors [2,3,4] the symplectic symmetry class shows an additional suppression of eigenvalues along the real axis, resulting into the double peak structure. The zero modes are driven away from the real axis for μ as small as $\mu = 0.000001$. This indicates that the limit $\mu \rightarrow 0$ is discontinuous.

Fig. 2 shows data for $ma = 20$ at strong non-Hermiticity, with $\mu = 0.2$ still below the phase transition. Here, the eigenvalues are rescaled with the square root of the volume, $\xi \sim z/\sqrt{d}$. Lacking an analytical prediction for the level spacing we have rescaled our eigenvalues by one parameter to fit Eq. (1). The normalized data nicely confirm the prediction, showing the correct symmetry.

4. Conclusions

We have tested the analytical predictions from a complex chiral symplectic matrix model using effectively quenched two color QCD. The agreement demonstrates that also at $\mu \neq 0$ matrix models are an excellent tool to describe the different gauge theory symmetry classes. In this preliminary study we have established the correct qualitative behavior from quenched data. A detailed analysis including different lattice volumes, scaling, and dynamical flavors with small mass is in progress.

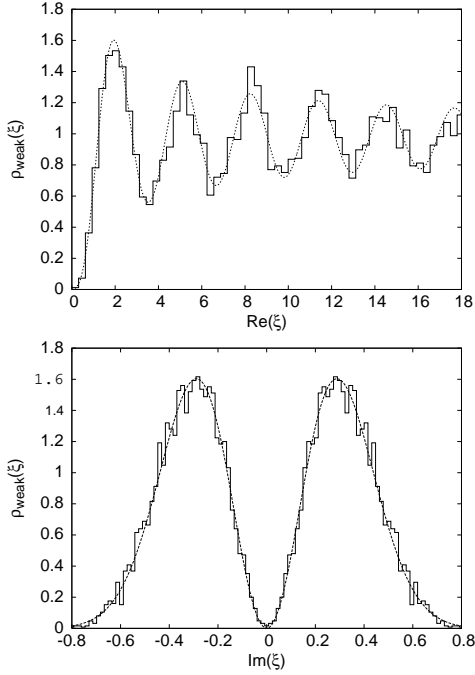


Figure 1. Data (histograms) for $V = 6^4$ at $\mu = 0.001$ vs. Eq. (1) for weak non-Hermiticity ($\alpha \sim 0.4$), cut parallel to the real axis along maxima (upper plot) and to the imaginary axis at the first maximum (lower plot).

Acknowledgments: Part of this work was supported by a DFG Heisenberg fellowship (G.A.). E.B. thanks the EU network HPRN-CT-1999-00161 EUROGRID – “Geometry and Disorder: from membranes to quantum gravity” for a post-doctoral grant.

REFERENCES

1. J.J.M. Verbaarschot and T. Wettig, *Ann. Rev. Nucl. Part. Sci.* 50 (2000) 343.
2. G. Akemann, *Phys. Rev. Lett.* 89 (2002) 072002; *J. Phys. A* 36 (2003) 3363.
3. K. Splittorff and J.J.M. Verbaarschot, *Nucl. Phys. B* 683 (2004) 467.
4. J.C. Osborn, hep-th/0403131.
5. G. Akemann, preprint SPhT T04/069.
6. G. Akemann and T. Wettig, *Phys. Rev. Lett.* 92 (2004) 102002.

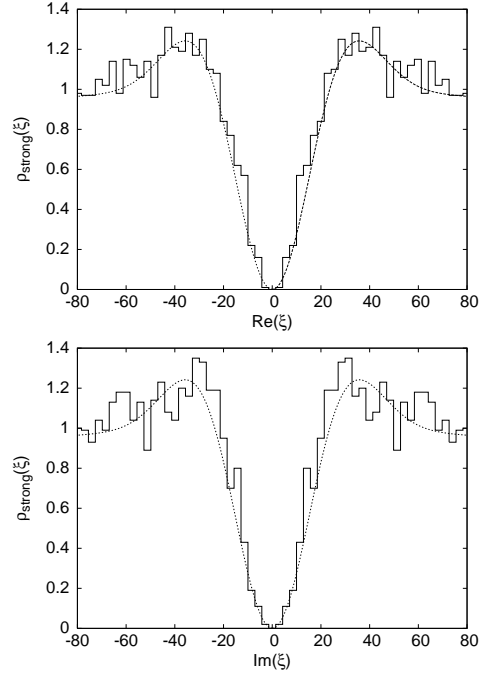


Figure 2. Data (histograms) for $V = 6^4$ at $\mu = 0.2$ vs. Eq. (1) for strong non-Hermiticity ($\alpha \sim 40$), cut along the real (upper plot) and imaginary (lower plot) axes.

7. S. Hands, J.B. Kogut, M.-P. Lombardo, and S.E. Morrison, *Nucl. Phys. B* 558 (1999) 327.
8. E. Bittner, M.-P. Lombardo, H. Markum, and R. Pullirsch, *Nucl. Phys. B (Proc. Suppl.)* 94 (2001) 445.
9. E. Bittner, M.-P. Lombardo, H. Markum, and R. Pullirsch, *Nucl. Phys. B (Proc. Suppl.)* 106 (2002) 468; *Spec. Issue Nucl. Phys. A* 702 (2002) p12.
10. M.A. Stephanov, *Phys. Rev. Lett.* 76 (1996) 4472.
11. M.A. Halasz, J.C. Osborn, and J.J.M. Verbaarschot, *Phys. Rev. D* 56 (1997) 7059.
12. Y.V. Fyodorov, B.A. Khoruzhenko, and H.-J. Sommers, *Phys. Lett. A* 226 (1997) 46; *Phys. Rev. Lett.* 79 (1997) 557.
13. J.B. Kogut, M.A. Stephanov, D. Toublan, J.J.M. Verbaarschot, and A. Zhitnitsky, *Nucl. Phys. B* 582 (2000) 477.
14. E. Follana, A. Hart, and C.T.H. Davies, hep-lat/0406010.